

Measurement of inherent material density of nanoparticle agglomerates

Kihong Park, David B. Kittelson, Michael R. Zachariah and Peter H. McMurry*

*Department of Mechanical Engineering, University of Minnesota, Minneapolis, MN 55455, USA; *Author for correspondence (E-mail: mcmurry@me.umn.edu)*

Received 30 December 2003; accepted in revised form 1 March 2004

Key words: inherent material density, instrumentation, agglomerates, diesel soot, aluminum nanoparticle, aerosol particle mass analyzer, instrumentation

Abstract

We describe a new technique to measure the size dependent inherent material density of chain agglomerate particles. Measurements were carried out for diesel soot and aluminum/alumina agglomerate particles in the nanometer size range. Transmission electron microscopy was used to measure the volumes of agglomerate particles that were preselected by mass using an aerosol particle mass analyzer. We found that the density of diesel exhaust particles increased from 1.27 to 1.78 g/cm³ as particle mobility size increased from 50 to 220 nm. When particles are preheated to remove volatile components, the density was 1.77 ± 0.07 g/cm³, independent of particle size. The densities measured after heating correspond to the inherent material density of diesel soot. Measurements with aluminum nanoparticles were made downstream of a furnace where aluminum (Al) was converted to alumina (Al₂O₃). From measurements of inherent material density we were able to infer the extent of reaction, which varied with furnace temperature.

Nanoparticles are increasingly of interest due to their potential effects on human health, their formation in the atmosphere by nucleation and eventual growth to sizes that can serve as cloud condensation nuclei, their use as precursors in the synthesis of nanophase materials, and their role as a source of contamination during the fabrication of semiconductor devices. It is now possible to routinely measure size distributions down to 3–5 nm (Ziemann et al., 1995; McMurry et al., 2000), and there has been significant recent progress in the measurement of nanoparticle composition (Reents & Ge, 2000; Kane et al., 2001; Tobias et al., 2001; Mahadevan et al., 2002; Voisin et al., 2003; Smith et al., 2004). Techniques for measuring the ‘effective’ density (mass divided by volume based on mobility diameter) are also established (Kelly & McMurry, 1992; Hering & Stolzenberg, 1995; McMurry et al., 2002), but the effective

density is typically significantly lower than the inherent material density for nonspherical particles. The inherent material density is a fundamental property of aerosol particles that can be used to place bounds on composition and that affects particle transport in gases. Inherent densities of bulk deposited samples for arbitrarily-shaped particles can be obtained from independent measurements of mass and volume by gas pycnometry (Hanel, 1977), but this approach typically requires several days to acquire a sufficient sample, and typically provides no information on size-dependent properties.

Here we employ a new approach to determine the inherent material density of agglomerates that consist of spherical primary nanoparticles. The differential mobility analyzer (DMA)-aerosol particle mass analyzer (APM) technique (McMurry et al., 2002; Park et al., 2003) is used to determine

the mass of mobility-classified particles that are subsequently analyzed by transmission electron microscopy (TEM).

Details of our experimental setup can be found in our previous papers (McMurry et al., 2002; Park et al., 2003). Briefly, particles are brought to Boltzmann equilibrium with a Po-210 neutralizer before they enter the DMA. The DMA (Knutson & Whitby, 1975) selects particles of a known mobility size which are then sent to the APM (Ehara et al., 1996). The APM consists of two cylindrical electrodes that rotate together about their common axis at a controlled speed. A voltage is applied to the inner electrode with the outer electrode grounded. Particles are introduced into the small gap between two electrodes and experience centrifugal and electrostatic forces that act in opposite directions. The APM transmits particles of a known mass (independent of particle shape or composition), determined by the balance of these forces. The governing equation describing this force balance is

$$m r \omega^2 = q \frac{V}{r \ln(r_2/r_1)} \quad (1)$$

where m is particle mass, ω is the APM angular speed, r is the radial location of particles relative to the axis of rotation, q is the particle charge, r_1 and r_2 are the radii of inner and outer electrodes, and V is the applied voltage. Using a low pressure impactor (LPI) (Hering et al., 1979), the mobility and mass classified particles are deposited on copper 200 mesh TEM grids coated with carbon or silicon monoxide films. A JEOL 1210 TEM (accelerating voltage: 40–120 kV, magnification: 50×–800,000×) was used to obtain the TEM images. The volume of the mass-classified particles was determined by analyzing particle images obtained with the TEM. The inherent material density equals the particle mass (from APM) divided by this volume.

Diesel soot nanoparticles were produced using either a John Deere diesel engine (John Deere 4045, 4 cylinder, 4.5l, 75 kW) or an Isuzu diesel engine (Isuzu, 3 cylinder, 1.5l, 10 kW) and a ejector-type two stage variable residence time dilution system (VRTDS) was employed to dilute diesel exhaust with clean, cool air (Abdul-Khalek et al., 1999). The VRTDS yielded primary dilution ratio of 16:1 and dilution temperature of 36°C for the John Deere engine, and 10:1 and 34°C for the Is-

uzu engine. The residence time in the VRTDS is approximately 2 s. Experiments were performed at a constant engine speed of 1400 rpm (John Deere) or 1800 rpm (Isuzu) at an engine load of 50% (John Deere) or 0% (Isuzu) with EPA fuel (~360 ppm S) and with a commercially available 15W-40 lubricating oil. Aluminum nanoparticles were generated by atomizing commercial aluminum nanopowder (Aveka Inc.) dispersed in methanol, and a furnace was used to oxidize the aluminum particles in air for known time (~1 s) and temperature (300 – 1100 °C).

Figure 1(a) shows typical morphologies of diesel soot particles deposited after DMA–APM system with a mobility diameter of 150 ± 22 nm and mass of 0.966 ± 0.310 fg. We observed that most soot particles are agglomerates of primary nanoparticles. The TEM image analysis includes measurements of primary particle diameter (d_p) and primary particle projected area (A_p). Measurements of the projected area (A_a), maximum projected length (L), and maximum projected width (W) of the agglomerates were made as shown in Figure 1(b). We observed that the mean primary particle diameter is 31.9 nm with a standard deviation of 7.2 nm and that primary particles of diesel agglomerates can be reasonably approximated by a normal distribution. The average values of the maximum length (L_{avg}), width (W_{avg}), and axial ratio ($(L/W)_{avg}$) with standard deviations, and the mode of projected area diameter ($D_{project}$) are shown in Table 1. A previous study (Rogak & Flagen, 1993) showed that projected area diameters of TiO₂ and Si agglomerates are nearly equal to mobility diameters in the free molecular regime, and the constant relationship between the projected area diameter and mobility diameter still holds throughout the transition regime ($D_{mobility} < 400$ nm). Our results show that this also applies to diesel particles in the 50–220 nm mobility diameter range. Figure 2 shows the morphology of aluminum particles with a mobility diameter of 100 ± 15 nm and mass of 0.554 ± 0.210 fg. These particles are also agglomerates that consist of spherical primary nanoparticles.

The mass of diesel soot particles as a function of mobility size measured with the DMA–APM is shown in Figure 3. In previous studies with spherical particles of known composition we showed that the mass of mobility-classified

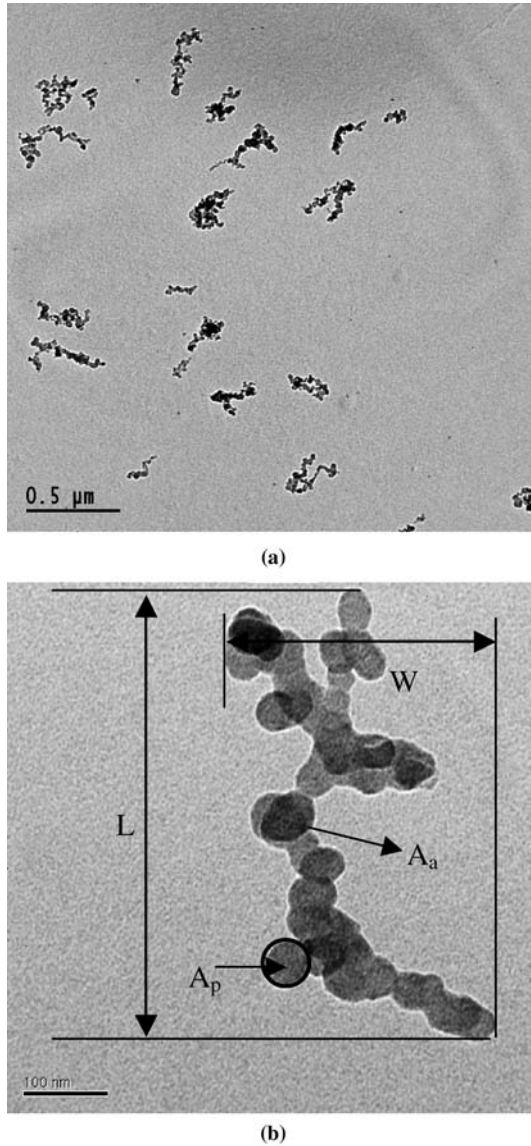


Figure 1. (a) TEM picture with a mobility diameter of 150 ± 22 nm and mass of 0.966 ± 0.310 fg for diesel soot particles (Isuzu engine, 0% load, 1800 rpm, EPA fuel (360 ppm S)). (b) Major parameters measured with the TEM: projected area (A_p) of primary particles, and projected area (A_a), maximum projected length (L), and maximum projected width (W) of the agglomerate.

particles can be measured to within 5% with the APM. Here we collected mass-classified particles on TEM grids and analyzed them by TEM. The number of primary particles in the agglomerates is determined after accounting for masking that

occurs when 2-dimensional projections of 3-dimensional particles are examined by TEM. We have used previously reported approaches to account for the masking (Samson et al., 1987; Meakin et al., 1989; Megaridis & Dobbins, 1990; Koçylu et al., 1995; Oh & Sorensen, 1997; Brasil et al., 1999). The mean volume for an ensemble of n mass classified particles is then

$$\bar{V} = \frac{\sum_i N_i \frac{\pi}{6} \bar{d}_p^3}{n} = \frac{\sum_i \left(k_a \left(\frac{A_a}{A_p} \right)^\alpha \right)_i \frac{\pi}{6} \bar{d}_p^3}{n} \quad (2)$$

where N_i is the number of primary particles in the agglomerate i , A_a is the projected area of the agglomerate, A_p is the projected area of primary particles, k_a is an empirical constant, and α is an empirical projected area exponent. In the present study, the values of α and k_a ($\alpha = 1.19$, $k_a = 1.81$) suggested by Oh and Sorensen (1997) are employed to determine the number of primary particles in diesel agglomerates. The volumes of diesel soot particles as a function of mobility size determined in this way are also shown in Figure 3, along with calculated values of inherent material density. Note that the inherent material density decreases from 1.78 ± 0.02 g/cm³ for particles larger than 100 nm to a value close to 1 g/cm³ at 50 nm. Figure 4 shows similar results that were obtained when particles were preheated to 300 °C prior to measurement. Note that in this case, the density is 1.77 ± 0.07 g/cm³, independent of particle size. We infer that the densities of the small particles increased due to the evaporation of condensed lubricating oil (density ~ 0.8 g/cm³) (Sakurai et al., 2003). Though the mixing characteristics of the condensed materials and non-volatile diesel soot depend on engine operating conditions, the intrinsic properties of diesel soot after removing condensed materials are probably fairly constant regardless of engine conditions. Thus, we conclude that the inherent material densities that were measured after heating are probably representative of values for diesel soot.

Similar measurements were made on aluminum agglomerate particles that had passed through an oxidizing furnace at various temperatures prior to mass measurement and collection. Results of these measurements are shown in Figure 5. Note that the inherent material density increased from ~ 2.7 to ~ 4 g/cm³ as the oven temperature increased. These values correspond closely to the density of

Table 1. Structural properties of diesel soot particles as a function of mobility diameter

D_{mobility} (nm)	Number of particles analyzed	D_{project} (nm) ^a	L_{avg} (nm)	W_{avg} (nm)	$(L/W)_{\text{avg}}$
50	157	45	61 ± 15	43 ± 7	1.5 ± 0.4
80	158	85	117 ± 22	61 ± 9	2.0 ± 0.6
100	305	95	155 ± 26	65 ± 10	2.5 ± 0.7
120	209	125	194 ± 37	80 ± 12	2.5 ± 0.8
150	159	145	238 ± 47	90 ± 15	2.8 ± 1.0
220	77	215	387 ± 77	119 ± 20	3.4 ± 1.2

^aThe projected area diameter (D_{project}) is evaluated at the center of the bin where the maximum count occurred. Diesel soot particles are produced from a John Deere (John Deere 4045) engine (50% load, 1400 rpm, EPA fuel (360 ppm S)).

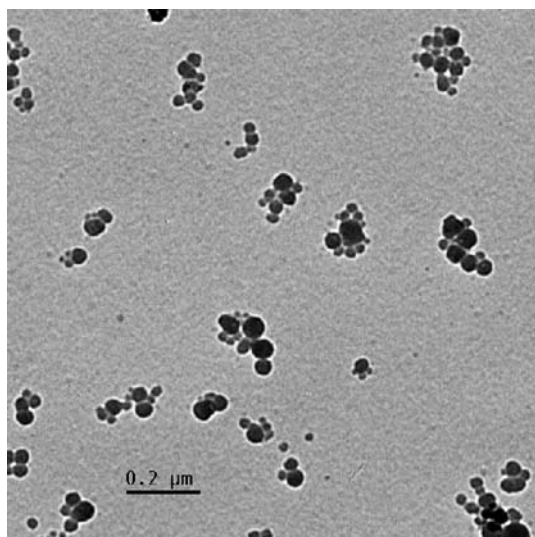


Figure 2. TEM picture of aluminum particles with a mobility diameter of 100 ± 15 nm and mass of 0.554 ± 0.210 fg. The aluminum particles are preheated to 300°C to remove the methanol solvent.

aluminum ($\sim 2.70 \text{ g/cm}^3$) and of aluminum oxide (Al_2O_3) (3.97 g/cm^3), suggesting that in this case the measured inherent density can be used to infer the extent of reaction. We also observe that the volume of particles for the given mobility size increased as the temperature increased, suggesting that agglomerates became more compact and denser.

In summary, we have demonstrated a new technique to measure the inherent density of agglomerate particles composed of primary nanoparticles. We show that the inherent density of the non-volatile components of diesel soot is $1.7\text{--}1.8 \text{ g/cm}^3$, and that the density of small

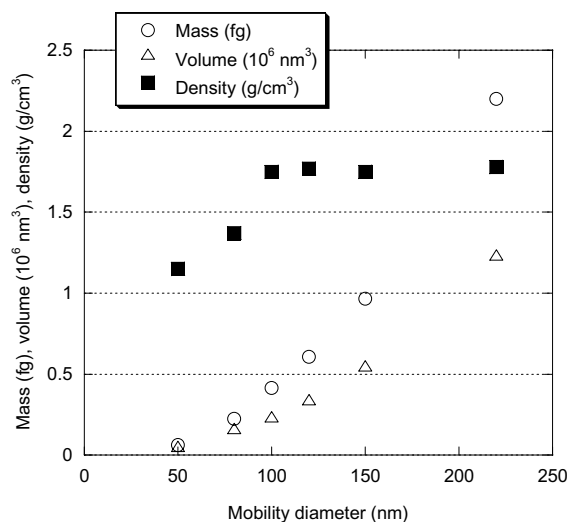


Figure 3. The inherent material density, mass, and volume of diesel soot particles as a function of mobility diameter. (John Deere engine, primary dilution ratio = 16:1, dilution temperature = 36°C , 50% load, 1400 rpm, EPA fuel (360 ppm S).)

(~ 50 nm) diesel exhaust particles approaches $\sim 1 \text{ g/cm}^3$ due to the presence of condensed material that can be removed by heating. We also show that measured densities of non-oxidized and oxidized aluminum agglomerates are in good agreement with expected values for aluminum and alumina suggesting that measurements of inherent material density obtained in this way could be used to infer the extent of reaction in aerosol reactors.

Acknowledgements

Although the research described in this article has been funded wholly or in part by the United States

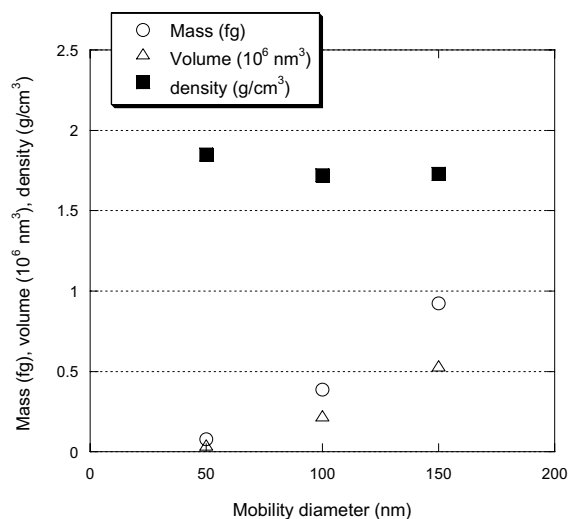


Figure 4. The mass, volume and inherent material density of diesel soot particles as a function of mobility diameter. Particles are preheated to 300 °C to remove condensed species. (Isuzu engine, primary dilution ratio = 10:1, dilution temperature = 34 °C, 0% load, 1800 rpm, EPA fuel (360 ppm S).)

Environmental Protection Agency through Grant Number R 826372-01-0 to the Georgia Institute of Technology and GIT Subcontract Number G-35-W62-G1 to the University of Minnesota, it has not been subjected to the Agency's required peer re-

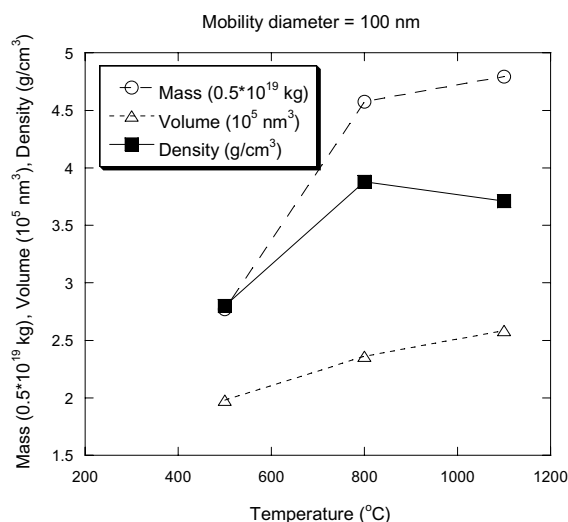


Figure 5. The dependence of mass, volume and inherent material density of aluminum particles following passage through a furnace at the indicated temperature.

view and therefore does not necessarily reflect the views of the Agency and no official endorsement should be inferred. We also acknowledge support from NSF Grant Number NSF/ATM-0096555.

References

- Abdul-Khalek I., D.B. Kittelson & F. Brear, 1999. The influence of dilution conditions on diesel exhaust particle size distribution measurements. *Soc. Automot. Eng.* 991142, 1–9.
- Brasil A.M., T.L. Farias & M.G. Carvalho, 1999. A recipe for image characterization of fractal-like aggregates. *J. Aerosol Sci.* 30, 1379–1389.
- Ehara K., C. Hagwood & K.J. Coakley, 1996. Novel method to classify aerosol particles according to their mass-to-charge ratio aerosol particle mass analyser. *J. Aerosol Sci.* 27(2), 217–234.
- Hanel G., 1977. Mean bulk densities of samples of dry atmospheric aerosol particles: a summary of measured data. *Pageoph.* 115, 799–803.
- Hering S.V. & M.R. Stolzenberg, 1995. On-line determination of particle size and density in the nanometer size range. *Aerosol Sci. Technol.* 23, 155–173.
- Hering S.V., S.K. Friedlander, J.J. Collins & L.W. Richard, 1979. Design and evaluation of a new low pressure impactor. *2. Environ. Sci. Technol.* 13, 184–188.
- Kane D.B., B. Oktem & M.V. Johnston, 2001. Nanoparticle detection by aerosol spectrometry. *Aerosol Sci. Technol.* 34, 520–527.
- Kelly W.P. & P.H. McMurry, 1992. Measurement of particle density by inertial classification of differential mobility analyzer-generated monodisperse aerosols. *Aerosol Sci. Technol.* 17, 199–212.
- Knutson E.O. & E.R. Whitby, 1975. Aerosol classification by electric mobility: Apparatus, theory, and applications. *J. Aerosol Sci.* 6, 443–451.
- Koylu U.O., G.M. Faeth, T.L. Farias & M.G. Carvalho, 1995. Fractal and projected structure properties of soot aggregates. *Combust Flame* 100, 621–633.
- Mahadevan R., D. Lee, H. Sakurai & M.R. Zachariah, 2002. Measurement of condensed phase reaction kinetics in the aerosol phase using single-particle mass-spectrometry. *J. Phys. Chem. A* 106, 11083–11092.
- McMurry P.H., K.S. Woo, R.J. Weber, D. Chen & D.Y.H. Pui, 2000. Size distributions of 3 to 10 nm atmospheric particles: Implications for nucleation mechanism. *Philos. Trans. Roy. Soc. London A358*, 2625–2642.
- McMurry P.H., X. Wang, K. Park & K. Ehara, 2002. The relationship between mass and mobility for atmospheric particles: A new technique for measuring particle density. *Aerosol Sci. Technol.* 36, 227–238.
- Meakin P., B. Donn & G.W. Mulholland, 1989. Collisions between point masses and fractal aggregates. *Langmuir* 5, 510–518.

- Megaridis C.M. & R.A. Dobbins, 1990. Morphological description of flame-generated materials. *Combust. Sci. Technol.* 71, 95–109.
- Oh C. & C.M. Sorensen, 1997. The effect of overlap between monomers on the determination of fractal cluster morphology. *J. Colloid Interf. Sci.* 193, 17–25.
- Park K., C. Feng, D.B. Kittelson & P.H. McMurry, 2003. Relationship between particle mass and mobility for diesel exhaust particles. *Environ. Sci. Technol.* 37, 577–583.
- Reents W.D. & Z. Ge, 2000. Simultaneous elemental composition and size distributions of submicron particles in real time using laser atomization/ionization mass spectrometry. *Aerosol Sci. Technol.* 33, 122–134.
- Rogak S.N. & R.C. Flagen, 1993. The mobility and structure of aerosol agglomerates. *Aerosol Sci. Technol.* 18, 25–47.
- Sakurai H., K. Park, P.H. McMurry, D.D. Zarling, D.B. Kittelson & P.J. Ziemann, 2003. Size-dependent mixing characteristics of volatile and non-volatile particles in diesel exhaust aerosols. *Environ. Sci. Technol.* 37, 5487–5495.
- Samson R.J., G.W. Mulholland & J.W. Gentry, 1987. Structural analysis of soot agglomerates. *Langmuir* 3, 272–281.
- Smith J.N., K.F. Moore, P.H. McMurry & F.L. Eisele, 2004. Atmospheric measurements of sub-20 nm diameter particle chemical composition performed using thermal desorption chemical ionization mass spectrometry. *Aerosol Sci. Technol.* 38(2), 100–110.
- Tobias, H.J., D.E. Beving, P.J. Ziemann, H. Sakurai, M. Zuk, P.H. McMurry, D. Zarling, R. Waytulonis & D.B. Kittelson, 2001. Chemical analysis of diesel engine nanoparticles using a nano-DMA/thermal desorption particle beam mass spectrometer. *Environ. Sci. Technol.* 35, 2233–2243.
- Voisin D., J.N. Smith, H. Sakurai, P.H. McMurry & F.L. Eisele, 2003. Thermal desorption chemical ionization mass spectrometer for ultrafine particle chemical composition. *Aerosol Sci. Technol.* 37, 471–475.
- Ziemann P.J., P. Liu, N.P. Rao, D.B. Kittelson & P.H. McMurry, 1995. Particle beam mass spectrometry of submicron particles charged to saturation in a electron beam. *J. Aerosol Sci.* 26, 745–756.